WELDING RESEARCH

SUPPLEMENT TO THE *WELDING JOURNAL*, MARCH 1991

Sponsored by the American Welding Society and the Welding Research Council

Correlation of Joint Penetration with Electron Beam Current Distribution

An empirical relationship for joint penetration as a function of beam width is proposed

BY G. K. HICKEN, W. H. GIEDT AND A. E. BENTLEY

ABSTRACT. Electron beam welding machine current distributions in the plane of the workpiece surface were measured by oscillating the beam across a narrow slit above a current collector. The beam focus location was varied from 2.54 cm (1 in.) above to 2.54 cm below the workpiece surface for beam currents of 4, 8 and 12 mA at 110 kV. Immediately following each beam current distribution measurement a bead-on-plate weld was made in 304L stainless steel.

Welding results demonstrated quantitatively the strong effect of beam focus location on penetration, and that it is necessary to control beam focus coil current to within $\pm 1\%$ to achieve $\pm 5\%$ accuracy in joint penetration. A procedure for evaluating a characteristic beam width from the beam profile data was developed, and a correlation of the penetration data in terms of a beam width, which includes 95% of the current, is presented.

KEY WORDS

EB Weld Penetration
Electron Beam Welding
EB Current Distribution
Electron Beam Focus
Gaussian Distribution
Fusion Zone Geometry
Slit Faraday Cup
Characteristic Beam Width
EB Distribution Measurement

Introduction

For a specified beam current and accelerating voltage, maximum penetration during electron beam welding is usually achieved when the beam is focused slightly below the workpiece surface. The focus coil current is determined by first adjusting the focus coil current until the apparent size of the beam impinging on a test surface at the same level as the workpiece surface is minimized. This is considered to be the focus current required for the beam to be focused at the workpiece surface. The focus coil current is then reduced to move the focus location below the surface. The amount of the reduction is usually decided by the operator based on his experience and judgment. This is clearly a qualitative procedure and usually involves some trial and error testing.

Comprehensive studies of the effects of beam focus location on joint penetration and fusion zone geometry (*i.e.*, the depth-to-width ratio) were carried out by Adams for low- and high-voltage welding machines (Refs. 1 and 2). The effects of accelerating voltage, beam current, welding speed and focus coil current were investigated. Beam current distributions were determined by moving the beam across a small tungsten wire probe 0.010 cm (0.004 in.) in diameter. The beam focus current yielding maximum penetration in 1.27-cm (0.5-in.) thick specimens of an austenitic stainless steel En 58J was defined as the optimum focus current (OFC). Illustrative results for an accelerating voltage of 130 kV and a beam current of 10 mA from a ribbon-type filament at a travel speed of 2.54 cm/s (60 in./min) and a work distance of 15.24 cm (6 in.) showed that maximum joint penetration was achieved with the beam focused about 2.54 cm (1.0 in.) below the workpiece

G. K. HICKEN and A. E. BENTLEY are members of the Technical Staff, and W. H. GIEDT is a Consultant, Process Development and Fabrication Division, Sandia National Laboratories, Livermore, Calif.

Paper presented at the 69th Annual AWS Meeting, held April 17-22, 1988, in New Orleans, La.

surface. However, when focused at the surface, the decrease in penetration was only about 4%. In contrast, with a hairpin-type filament, optimum or maximum penetration occurred with the beam focused at the workpiece surface, and a 3% change from OFC reduced the penetration to about one-half of optimum. It was concluded that for accurate control of penetration with a ribbon filament it would be necessary for the focus current to be within ±1% of the OFC value. Greater precision would be required with a hairpin-type filament.

The results of the studies reported in Refs. 1 and 2 clearly establish the importance of beam focus location. Beam current density distributions, as indicated by moving the beam across a small wire, were utilized to determine the beam focus location, and joint penetration was shown to be dramatically changed by varying the beam focus location relative to the upper surface of the workpiece. However, no consideration was given to investigating whether or not a quantitative relationship exists between beam current distribution at a workpiece surface and penetration. This was the objective of the study described herein.

Beam Current Density Distribution Measurement Techniques

A number of methods for investigating the current distribution in a highly focused EB have been developed. The most familiar involves the use of a small-diameter wire probe. As mentioned above, Adams moved the beam across the wire. Others have swung the wire or wires through the beam to eliminate possible perturbation of the beam by the deflection coil. This approach and its limitations are described by Hartwig and Hopwood (Ref. 3).

The output of a wire probe at any location in a beam represents a summation of the current through the projected area of the wire at that location. The resulting profile as the wire sweeps through the beam may therefore be regarded as one-dimensional. Traverses in different directions generally show some variation, indicating that the beam is not symmetrical. The two-dimensional nature of beams has been investigated by making a series of measurements in two directions with a small aperture in a plate (Refs. 3–5). Mapping of the current density field in this way requires continuous exposure of the plate area around the aperture to the intense beam. This results in substantial heating of the plate. Hence, reported measurements have been for relatively low beam power or current levels.

A technique yielding results similar to a wire probe is to form a narrow slit between two plates (Ref. 6). While the slit is moved under or the beam is moved over the slit, the electrons passing through the slit are collected in a Faraday cup below. This type device can withstand exposure to higher current beams and was therefore selected for this investigation. It is described in the following section.

Experimental Apparatus and Procedure

The device fabricated for electron beam current distribution measurements is illustrated in Fig. 1. The electron beam is oscillated across the opening formed between two tungsten plates mounted on top of a copper body, which acts as a heat sink. At any instant, a fraction of the beam passes through the narrow slit formed at the base of the tungsten plates. The remainder is collected on the plates and flows through the copper body to the ground. As the beam moves across the opening between the tungsten plates, the variation in the electron flow through the slit is a measure of the current density distribution in the beam.

The electrons that pass through the narrow slit then pass through a 0.635-cm (0.25-in.) diameter channel, are collected in a cupped copper cylinder (the Faraday cup), and flow through a 100-ohm resistor to the ground. The voltage drop across this resistor was digitized at 0.5-μs intervals and recorded.[1] The current variation with location (equal to the beam oscillation velocity multiplied by the time measured from the start of current flow to the Faraday cup) can then be evaluated from the record of the voltage drop across the resistor.

The narrow slit for making beam current profile measurements is formed between two 0.95-cm (0.5-in.) thick tungsten plates. As shown, the inner faces of these plates are machined to an angle of 10 deg. This tapering provides sharp edges for accurately defining the beam sampling width. Tapering also increases the surface area over which the rest of the beam impinges. This spreads the heating effect of the beam through the thickness of the tungsten plates in the critical region near the edges of the slit. The slit width was set with a feeler gauge. Ideally, the narrower the opening, the better. Practically, however, the current signal must be sufficiently greater than the noise level to obtain acceptable measurements. This will depend on the beam current and the size of the beam. Results indicate that an opening as small as 0.0025 cm (0.001 in.) is satisfactory for a sharply focused high-voltage beam. As a general specification, it is suggested that the opening be 10% or less of the beam full width, which includes 95% of the total power.

Initial tests were conducted with a model W4 Hamilton Standard welding machine (with a ribbon filament) by mov-

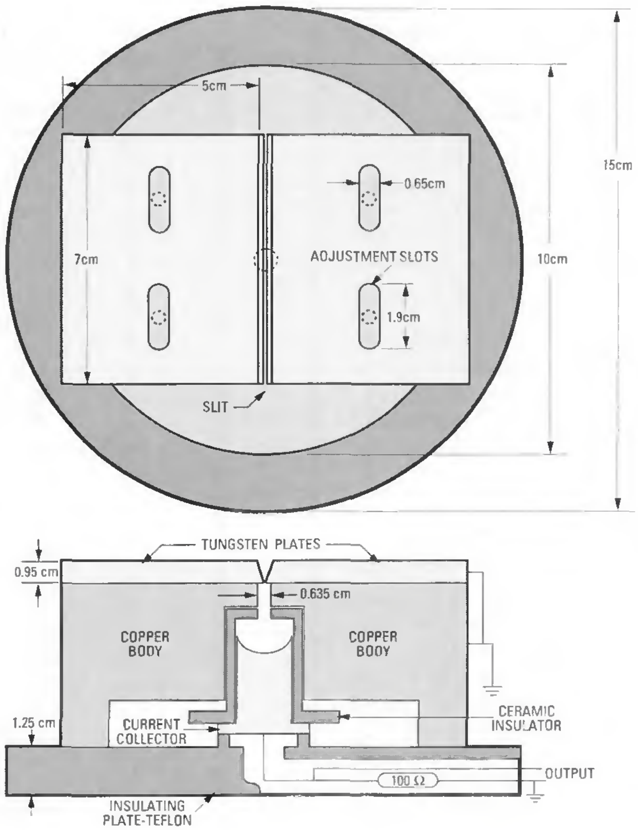

Fig. 1 — Narrow-slit Faraday cup.

1. *A Model 4094 Nicolet oscilloscope was used with a Model 4562 processing unit.*

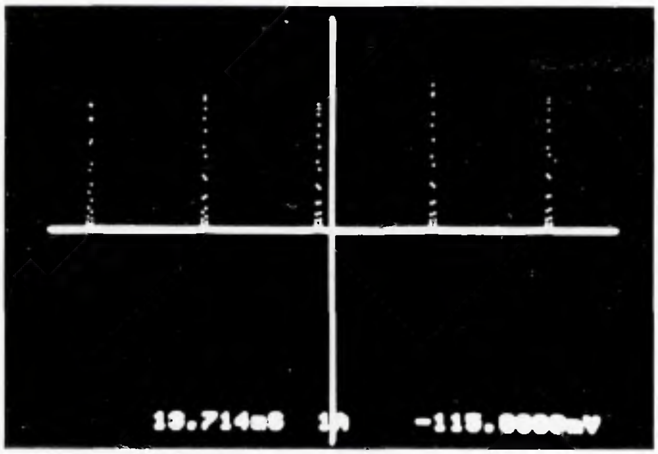

Fig. 2 — Illustrative record of a series of electron beam current distributions for surface focus at 110 kV and 4 mA.

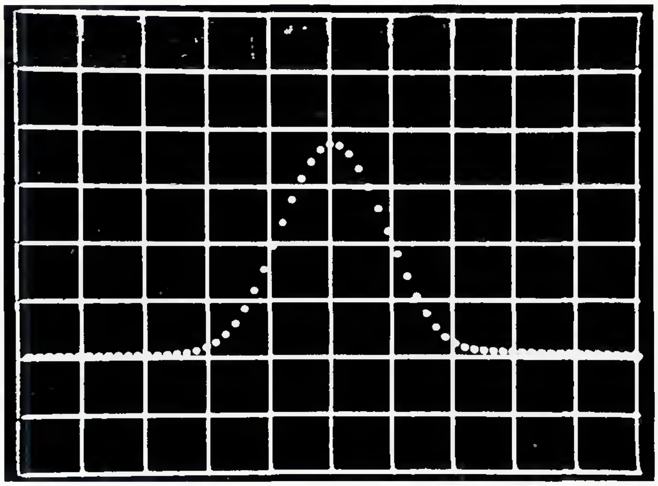

Fig. 3 — Photograph of single expanded current distribution from Fig. 2.

ing the slit under the beam at speeds of 2.5 and 3.81 cm/s (60 and 90 in./min). Melting of the knife edges occurred at a current of 8 mA. To minimize heating during final testing, the beam was oscillated at a frequency of 150 Hz and total amplitude of about 0.75 to 1.0 cm across the slit, while the slit was moved normal to the direction of oscillation at 3.81 cm/s (90 in./min). In this way, a record of approximately 10 to 15 profiles was obtained for each test condition. Part of a typical record is shown in Fig. 2. No melting of the knife edges occurred up to currents of 12 mA. The slit opening was positioned 15.24 cm (6 in.) below the focus coil heat shield. The effect of beam focus was investigated by focusing the beam at locations varying from 2.5 cm (1.0 in.) above to 2.5 cm below the upper surface of the weld specimen surface. Focus location was determined in the usual way, *i.e.*, minimizing the beam spot size when impinging on a tungsten surface at the selected elevation. All profiles were measured with the slit 15.24 cm (6 in.) below the heat shield.

After records of the beam profiles were obtained both normal and parallel to the travel direction, a bead-on-plate weld was made on 304L stainless steel specimens 0.635 cm (0.25 in.) thick for the 4- and 8-mA tests and 0.9525 cm (0.375 in.) thick for the 12-mA tests. The test plates were mounted so that the upper surfaces were at the same level as the slit opening, *i.e.*, the work distance was 15.24 cm.

Results

Electron beam profiles and weld penetrations in 304L stainless steel were measured with the beam focused at distances of 12.7, 14, 14.6, 15.24, 15.9, 16.5 and 17.8 cm (5, 5.5, 5.75, 6, 6.25, 6.5 and 7 in.) below the heat shield. For each test condition, as the beam was being oscillated parallel to the travel direction across the slit and the slit was being moved normal to the beam oscillation direction, a record of approximately 10 to 15 beam profiles was obtained. Figure 2 shows part of a record for surface focus at 110 kV and 4 mA. Note that there is about $\pm 5\%$ variation in the peak values. Similar variations were observed at other current levels. Although the source of these fluctuations has not been determined, it is recognized that they could be responsible for variations in the root region of welds. An expanded view of a single profile from the record in Fig. 2 is presented in Fig. 3. The slit opening was set at 0.010 cm (0.004 in.). The individual points represent the voltage drop across the 100-ohm resistor at 5 μs intervals (Δt). The velocity of the beam crossing the slit was about 300 cm/s. Each datum point (Fig. 3) is determined by the oscillograph circuitry in a sampling time of about one nanosecond. During this time, the beam would move less than 0.1% of the slit width. Hence, the data points shown are essentially instantaneous values and represent the current through the slit as a function of beam location. Rotating the slit 90 deg and oscillating the beam normal to the travel direction yielded amost identical results, indicating that the distribution was close to symmetrical.

Assuming that the beam current has a probability distribution that can be represented by a Gaussian density function, the current density would be given by

$$I(r) = (I/2\pi\sigma_s^2)\exp(-r^2/2\sigma_s^2) \quad (1)$$

where I(r) represents the current per unit

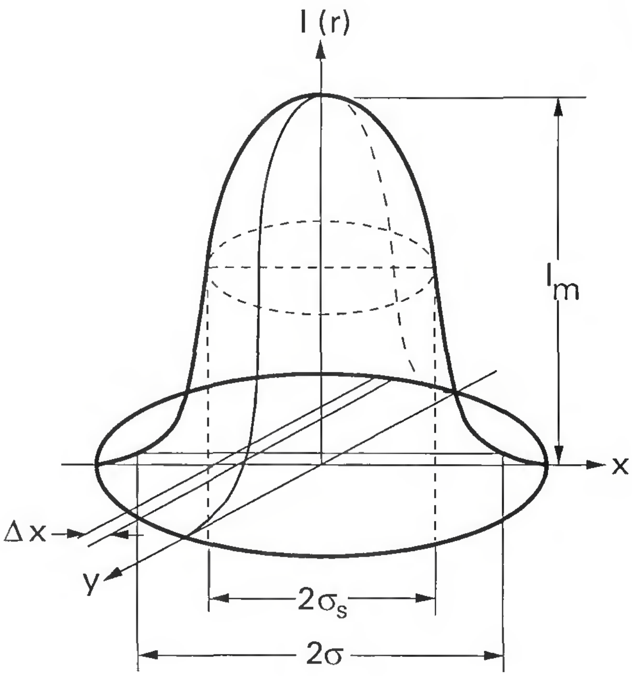

Fig. 4 — Gaussian distribution function.

area at a radius r (Fig. 4), I the total beam current, and the distribution parameter σ_s is the standard deviation. To compare this distribution with measurements such as shown in Fig. 3, it is necessary to integrate Equation 1 in one coordinate direction (*e.g.*, in the y direction) from $-\infty$ to $+\infty$ (Fig. 4). Introducing $r^2 = x^2 + y^2$,

$$I(r) = (I/2\pi\sigma_s^2) \exp[-(x^2 + y^2)/2\sigma_s^2] \quad (2)$$

Integrating in the y direction will yield an expression for current through an area equal to slit width Δs and extending from $-\infty$ to $+\infty$. This will be denoted as slit current $I_s(x)$ and is equal to the one-dimensionally integrated current density I(x) times slit width Δs. So, $I_s(x)$ denotes (assuming as suggested in Fig. 4 that $\Delta s << \sigma_s$)

$$I_s(x) = I(x)\Delta s = \int_{-\infty}^{+\infty}(I/2\pi\sigma_s^2) \exp [-x^2 + y^2)/2\sigma_s^2]\Delta s dy$$

This gives

$$I(x)\Delta s = (I/\sqrt{2\pi\sigma_s}) \exp[-x^2/2\sigma_s^2]\Delta s \quad (3)$$

or

$$I(x) = (I/\sqrt{2\pi\sigma_s})\exp[-x^2/2\sigma_s^2] \quad (4)$$

in which typical units for I(x) would be mA/mm.

To determine the value of σ_s, the distribution of integrated current density $I(x_i)$ was first calculated by dividing the measured voltage distribution data points by the product of the resistance in the Faraday cup circuit and the slit width. These values were then normalized by dividing by the total beam current, yielding a set of values of $i(x_i) = I(x_i)/I$. The first and second moments, M(x) and $M(x^2)$ were then calculated as

$$M(x) = \sum_{i=1}^{n} x_i i(x_i)\Delta x \quad (5)$$

$$M(x^2) = \sum_{i=1}^{n} x_i^2 i(x_i)\Delta x \quad (6)$$

where $\Delta x = v\Delta t$ is the distance the beam moves between data points, $x_i = i\Delta x$, and n is the number of data points. The standard deviation σ_s is then given by

$$\sigma_s^2 = [M(x^2) - M(x)^2] \quad (7)$$

For each test condition, values of σ_s for nine consecutive beam profiles were evaluated and an average value then determined.

Recognizing that the effective area of the beam will be larger than the area within a radius equal to the standard distribution parameter σ_s, the radius σ defining the area within which 95% of the current flows was introduced. This distribution parameter is commonly used in describing welding heat sources and is related to σ_s by

$$\sigma^2 = 6\sigma_s^2 \quad (8)$$

Substituting this in Equation 4 gives

$$I(x) = \sqrt{(3/\pi)}(I/\sigma)\exp[-3(x/\sigma)^2] \quad (9)$$

The measured one-dimensional distribution of the beam current for the beam focused 0.635 cm below the specimen surface is compared in Fig. 5 with the distribution predicted from Equation 9 using the value of σ determined from the data. The agreement is considered exceptionally good. A similar comparison is shown in Fig. 6 for the beam focused 2.5 cm below the specimen surface. Note that the measured distribution is not symmetrical, and that the peak of the Gaussian distribution is about 10% higher than the experimental data.

The beam width as characterized by σ is also shown in Figs. 5 and 6. Variations of this distribution parameter with beam focus current for distributions measured at the specimen surface are plotted in Fig. 7 for beam currents of 4 and 8 mA. Note that there is very little difference between the values of σ for currents of 522 and 518 mA, which yielded focus at the surface and at 0.635 cm below the surface, respectively. This suggests that the joint penetrations produced for these two conditions would be about the same. The experimental penetration data presented in Fig. 8 show this to be true. Note that measured penetrations for the beam focused at the surface, 0.635 and 1.27 cm (0.25 and 0.5 in.) below are within a range of 6%.

In comparing measured beam profiles with predicted distributions from values of σ evaluated as described above, it was noted that for locations within about 0.25 in. above or below the focus plane, agreement was similar to that illustrated in Fig. 5. For distances greater than 0.25 in. from the focus plane, current distributions became increasingly more nonsymmetrical. This is due to the beam being elongated to an elliptical shape with the direction of the major axis falling between the travel (x) and the normal (y) directions. The small-aperture two-dimensional measurements presented in Ref. 3 illustrate this distribution. In view of this trend, it is recognized that characterizing the beam at locations beyond the focal plane region with a single distribution parameter will only be approximate. For the nonsymmetrical distributions observed, the possibility of using distribution parameters evaluated for both the x and y directions should be investigated.

The sensitivity of penetration to beam focus current is demonstrated in Fig. 9. Two sets of data for 8 mA and 110 kV are plotted. From the error band, including a

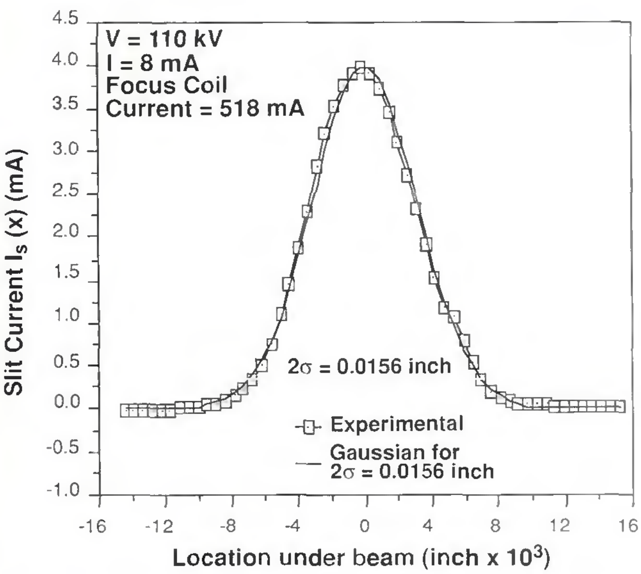

Fig. 5 — One-dimensional integrated beam current distribution in travel direction for focus 0.25 in. below workpiece surface.

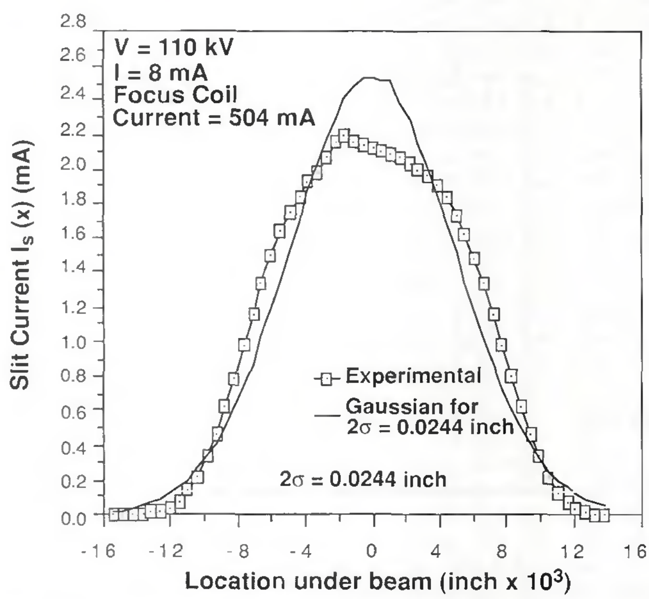

Fig. 6 — One-dimensional integrated beam current distribution in travel direction for focus 1.0 in. below workpiece surface.

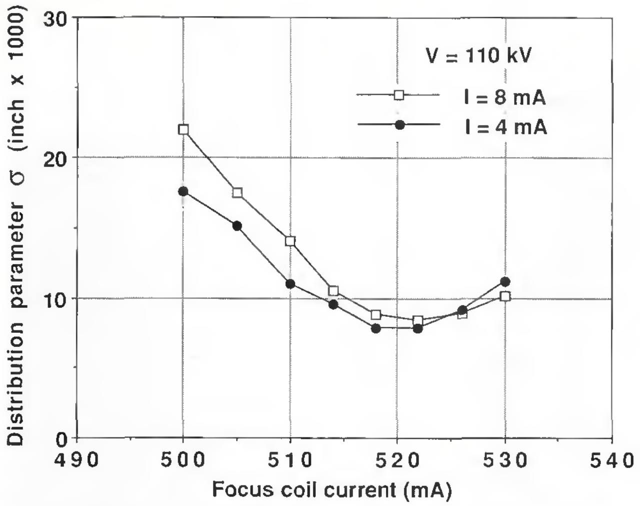

Fig. 7 — Beam current distribution parameter σ as a function of focus coil current.

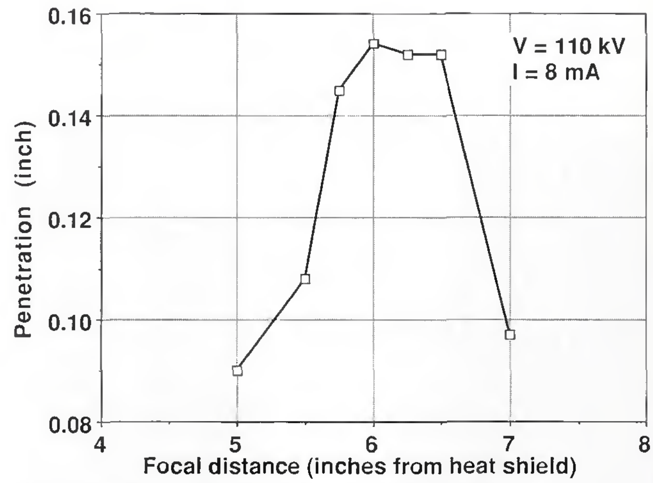

Fig. 8 — Variation of penetration with beam focus location.

$\pm 5\%$ variation in joint penetration, it can be seen that to satisfy such a requirement the beam focus coil current must be controlled to an accuracy of $\pm 1\%$.

Penetration Correlation Using Distribution Parameter

In Ref. 7, it was shown that the variation of the average power per unit of penetration (P/d), nondimensionalized by dividing by the product of the average thermal conductivity k_a and the melting temperature referenced to ambient Θ_m (that is, $(P/d)/k_a\Theta_m = Y$), could be described by a simple power function of the parameter $(vw/\alpha_a) = X_w$, where v is the welding speed, w the fusion zone width at the surface, and α_a the average thermal diffusivity.[2] This relation is given by

$$Y = 3.33 X_w^{0.625} \qquad (10)$$

and is plotted in Fig. 10. The data points represented by circles along this curve are based on measurements of penetration and fusion zone width at the surface for the test runs with the beam focused within ± 0.635 cm of the workpiece surface.[3] The deviations of the data from the curve are within $\pm 20\%$. As anticipated, deviations of results for beam focus at distances greater than 0.635 cm from the surface were greater than $\pm 20\%$ and were not included (the data points for these focus locations tend to fall above the curve of Equation 10, indicating that a higher power per unit of penetration is required).

The measured beam current distributions shown in Figs. 5 and 6 are superimposed on transverse sections of their respective fusion zones in Figs. 11 and 12. Note that near the surface the beam diameter as characterized by 2σ is about one-half of the fusion zone width. In a recent study Wei, *et al.* (Ref. 8), developed an iterative method for determining the shape of the vapor cavity for a beam with a Gaussian power density distribution. Their results indicate that the width of the vapor cavity near the surface is approximately equal to 2σ. Assuming this to be true, the additional width at the surface on each side shown in Figs. 11 and 12 (on the order of σ) would be indicative of the thickness of the liquid layer surrounding the vapor cavity. The indicated thickness is of the order of magnitude of liquid layer thickness predicted by Wei and Giedt (Ref. 9).

2. *The nondimensional energy transfer parameter $Y = P/dk\Theta_m$ can be identified as a Biot number when written as $(P/d^2\Theta_m)(d/k_a)$. The parameter $X_w = vw/a_a$ will be recognized as a Peclet number.*

3. *The average thermal property values selected for 304L stainless steel were $k_a = 0.25$ W/cm °C, $\Theta_m = T_m - T_\infty = 1408$ °C, and $\alpha_a = 0.045$ cm²/s.*

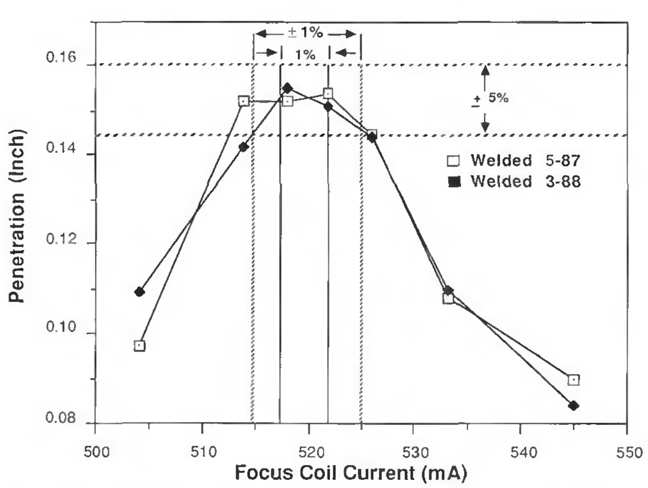

Fig. 9 — Variation of penetration with focus coil current for 110 kV and 8 mA.

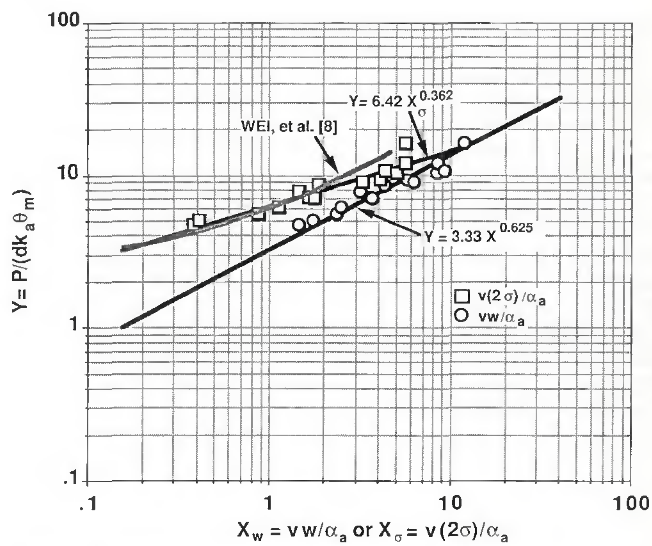

Fig. 10 — Correlation of partial penetration data.

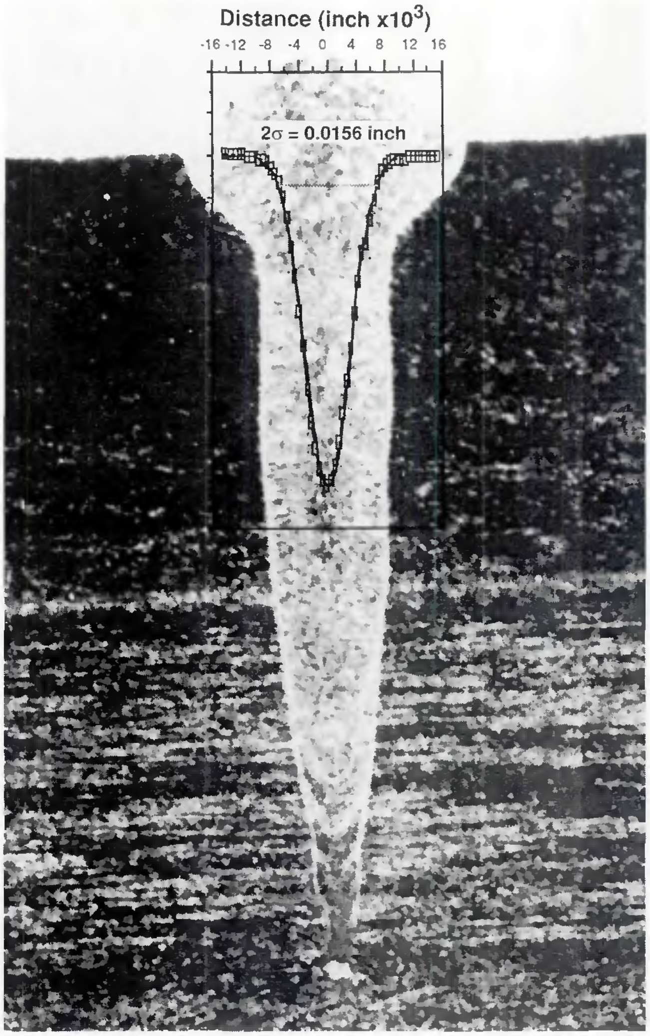

Fig. 11 — Comparison of beam current size with transverse fusion zone for 110 kV, 8 mA and focus 0.25 in. below workpiece surface.

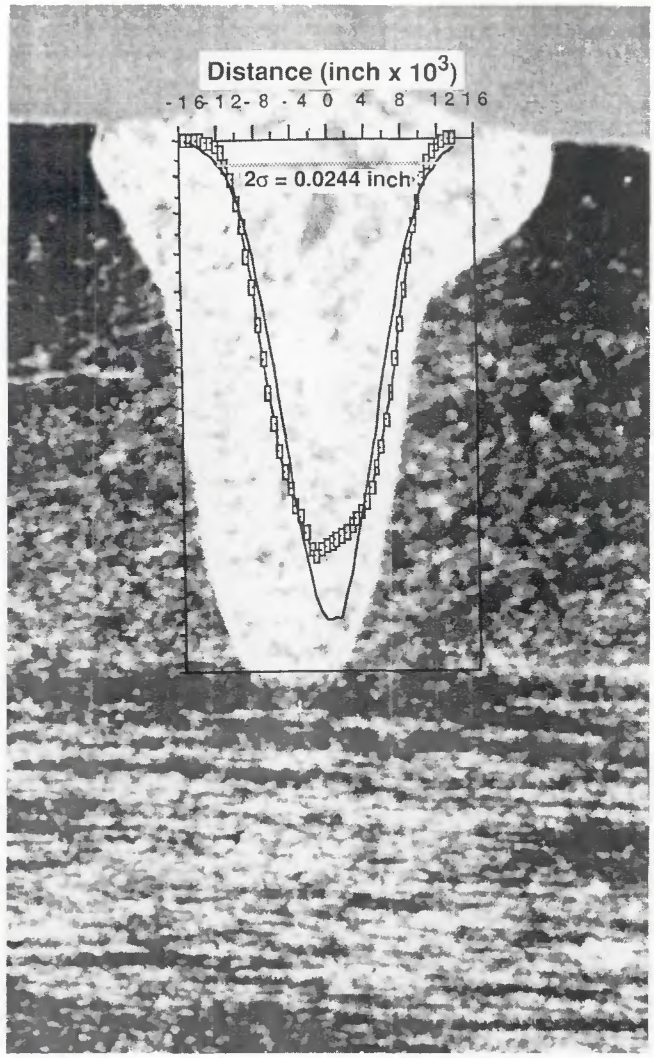

Fig. 12 — Comparison of beam current size with transverse fusion zone for 110 kV, 8 mA and focus 1.0 in. below workpiece surface.

These observations suggest that, similar to the use of the melt width w at the surface, σ may also be an appropriate width parameter to use in correlating EB penetration. The points plotted as squares in Fig. 10 represent the results with w in vw/α_a replaced by 2σ, *i.e.*, $Y = P/dk_a\Theta_m$ as a function of $X_\sigma = v(2\sigma)/\alpha_a$. A least squares fit of these data points yielded the relation

$$Y = 6.42X_\sigma^{0.362} \tag{11}$$

Scatter of the data about the curve of this equation is within $\pm 20\%$, which is similar to the deviations of the data from Equation 10. This indicates that if σ is known or determined from a beam profile measurement, joint penetration can be predicted from this relation as accurately as from Equation 10.

The possibility of correlating penetration during EB welding with a Gaussian distribution parameter is supported by the analytical predictions presented by Wei, *et al.* (Ref. 8). As shown, the curve representing his modified results (Ref. 10) in Fig. 10 essentially coincides with the curve for Equation 11 for values of $X_\sigma = v(2\sigma)/\alpha_a$ up to 2.0, and rises to about 25% above it as X_σ approaches 5.0. Additional calculations to extend the predictions to higher values of X_σ would be desirable.

As shown in Fig. 10, the curve of Equation 11 appears to intersect the $Y = 3.33\ X_w^{0.625}$ curve at about $X_w = 12$. The X_σ curve is not shown beyond this point because it is believed that the actual trend of the penetration with X_σ is to become parallel or asymptotic to the curve based on X_w. The latter possibility implies that as the variable $v(2\sigma)/\alpha_a$ increases, the quantity 2σ approaches the surface fusion zone width w. In either case, a more complex relation than Equation 11 may be needed to describe the variation of penetration with σ. However, since an upper limit of 12 for $X_\sigma = v(2\sigma)/\alpha_a$ includes most welding conditions, a simple relation such as Equation 11 may be adequate for a practical prediction of penetration from a measured beam width. Tests at higher values of $v(2\sigma)/\alpha_a$ are planned to investigate this hypothesis and to validate the proposed correlation given by Equation 11.

Conclusions

From the results of this study it was concluded that:

1) The current distribution in the region within about 0.635 cm above and below the focus location of a high-voltage electron beam is closely approximated by a Gaussian density function.

2) Beyond 0.635 cm from the focus location, the distribution becomes increasingly nonsymmetrical.

3) The current distribution in a focused electron beam at a workpiece surface can be measured and characterized with a one-dimensional survey of the beam with a narrow-slit Faraday cup.

4) Penetration is strongly dependent on beam focus location. With a ribbon-

type filament, an accuracy of ±1% in beam focus current is required to control penetration to within ±5%.

5) A beam Gaussian distribution parameter evaluated from a narrow-slit Faraday cup traverse can be used in Equation 11 to predict welding penetration with an accuracy of ±20%.

Acknowledgment

The investigation described in this paper was carried out at the Sandia National Laboratories, Livermore, Calif. The support of the United States Department of Energy under Contract DE-AC04-76D-P00789 is gratefully acknowledged.

References

1. Adams, M. J. 1963. Low voltage electron beam welding: effect on process parameters. *British Welding Journal* 52(3):134-142.

2. Adams, M. J. 1968. High voltage electron beam welding. *British Welding Journal* 57(9): 451-467.

3. Hartwig, C. M., and Hopwood, J. E. 1985. *Technique for Sampling Focused Electron Beam for Welding Application.* Sandia National Laboratories Report SAND85-8710, Livermore, Calif.

4. Sanderson. A. 1968. Electron beam delineation and penetration, *British Welding Journal* 15(10):509-523.

5. Motting, A., and Sepold, G. 1968. *Proceedings of Third Intl. Conf. on Electron and Ion Beam Science and Technology.* Electrochemical Society, N.Y. pp. 318-325.

6. Burghardt, P. 1989. *Evaluation of a Modified Faraday Cup.* Report RFP-4371, EGG Rocky Flats, Inc., Golden, Colo.

7. Giedt, W. H., and Tallerico, L. N. 1988. Prediction of electron beam depth of penetration. *Welding Journal* 67(12):299-s to 305-s.

8. Wei, P. S., Wu, T. H., and Chow, Y. T. 1990. Investigation of high-intensity beam characteristics on welding cavity shape and temperature distribution. ASME *Jour. of Heat Transfer* 112(1):163-169.

9. Wei. P. S., and Giedt, W. H. 1985. Surface tension gradient-driven flow around an electron beam welding cavity. *Welding Journal* 64(9):251-s to 259-s.

10. Wei, P. S. 1991. Personal communication to authors.